Simulation for Training Cochlear Implant Electrode Insertion

Xingjun Ma*, Sudanthi Wijewickrema†, Yun Zhou†, Bridget Copson†,
James Bailey*, Gregor Kennedy‡ and Stephen O'Leary†
* *Department of Computing & Information Systems, The University of Melbourne, Australia*
† *Department of Surgery (Otolaryngology), The University of Melbourne, Australia*
‡ *Center for the Study of Higher Education, The University of Melbourne, Australia*
Email: {xingjunm@student., swijewickrem@, yun.zhou@, bcopson@student., baileyj@, gek@, sjoleary@}unimelb.edu.au

***Abstract*—Cochlear implant surgery is performed to restore hearing in patients with a range of hearing disorders. To optimise hearing outcomes, trauma during the insertion of a cochlear implant electrode has to be minimised. Factors that contribute to the degree of trauma caused during surgery include: the location of the electrode, type of electrode, and the competence level of the surgeon. Surgical competence depends on knowledge of anatomy and experience in a range of situations, along with technical skills. Thus, during training, a surgeon should be exposed to a range of anatomical variations, where he/she can learn and practice the intricacies of the surgical procedure, as well as explore different implant options and consequences thereof. Virtual reality simulation offers a versatile platform on which such training can be conducted. In this paper, we discuss a prototype implementation for the visualisation and analysis of electrode trajectories in relation to anatomical variation, prior to its inclusion in a virtual reality training module for cochlear implant surgery.**

***Keywords*-Cochlear Implant Trajectory, Cochlear Implant Electrode Insertion Training, Electrode Trajectory Visualisation, Virtual Reality Simulation**

I. Introduction

Cochlear implants are increasingly being used to restore or augment hearing in patients with a variety of hearing disorders [1], [2]. They are designed to replace the functionality of a damaged inner ear. The external portion of a cochlear implant, placed behind the ear, typically consists of a microphone and speech processor that capture sound and convert it into digital code. The (internal) implant comprises a transmitter that converts the digital code to electrical impulses, and an electrode array that transfers them to different regions of the auditory nerve.

It is evidenced that to optimise hearing outcomes from cochlear implants, it is necessary to reduce the amount of trauma inflicted during the implantation process [3]. Location of the electrode is an important factor in trauma reduction [4], [5] which depends to a large degree on sufficient preparation of the temporal bone prior to the insertion [6], [7], [8]. As such, it is imperative that surgeons be trained in proper surgical preparation and exposed to a variety of anatomical variations so that they understand how a surgical procedure can be tailored according to the patient. Torres et al. [9] demonstrated that experts inserted the electrodes closer to the optimal insertion vector than fellows and residents, confirming the importance of experience and training in cochlear implantation.

Training in cochlear implant surgery is currently reliant on the apprenticeship model where a trainee observes and practices under expert guidance in the operating theatre and cadaveric training programs [10], [11]. However, the sole use of these training methods are becoming increasingly inefficient in the current climate due to reasons such as scarcity of cadavers and reduction in time available for teaching [12], [13]. Computer based simulation technologies such as virtual reality (VR) offer an attractive alternative to supplement traditional training methods. Use of VR simulation for skill acquisition and translation in temporal bone surgery such as cortical mastoidectomy has been well studied [14], [15], [16], [17], [18]. Recent studies such as Copson et al. [19] have also addressed how more complex surgeries such as preparation/dissection of the temporal bone for cochlear implantation can be trained.

VR simulation also offers a convenient platform to train surgeons on the electrode insertion part of cochlear implant surgery. One such example is Todd et al. [20], where visual and haptic feedback is provided to train electrode insertion to the cochlea. However, this simulation is quite limited in that it does not address how the dissection of the temporal bone and anatomical structures such as the facial nerve and chorda tympani affect the insertion vectors.

Here, we discuss a prototype simulation module that allows the trainee to visualise valid electrode trajectories along with their contact locations on the cochlea at different stages of temporal bone preparation. This will provide the opportunity to understand how the level of dissection affects the number of available trajectories, and how different strategies may be required for different anatomies. Integration of this system to a haptic-enabled VR simulator will allow the trainee to practice the actual electrode insertion guided by the possible trajectories thus generated.

The rest of the paper is organised as follows. Section II briefly describes the VR simulation platform for which this prototype is developed, along with details of cochlear implantation surgery. Sections III and IV discuss how the problem is formulated and the design of the proposed solution respectively. Section V shows examples of visualisation

and analysis of electrode trajectories using the proposed system. Section VI concludes the paper with a discussion of findings and future avenues of research.

II. Setting

A. Simulation Platform

The prototype system discussed here is intended for the University of Melbourne VR temporal bone surgery simulator (see figure 1). The simulator consists of a PC (or a laptop), a haptic device, and a MIDI controller to provide input. A virtual model of a temporal bone is displayed in 3D with which the surgeon interacts using the haptic device that provides force/tactile feedback. Time since the start of the surgery is displayed on the screen for ease of assessment and analysis.

Figure 1: The University of Melbourne VR temporal bone surgery simulator.

Anatomical structures of the middle and inner ear that have to be safely navigated when performing temporal bone surgery are presented in the virtual model (see figure 2).

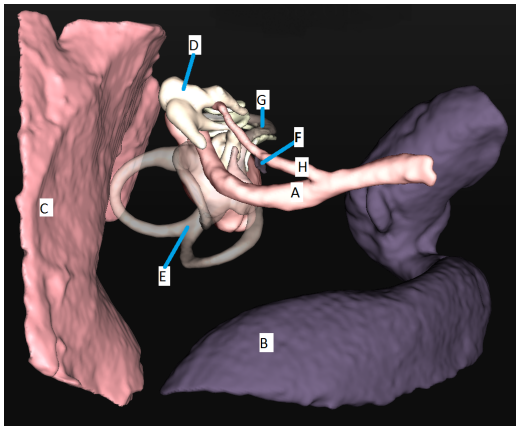

Figure 2: Anatomical structures of the middle and inner ear: A) facial nerve, B) sigmoid sinus, C) dura, D) ossicles, E) semicircular canals, F) round window, G) cochlea, and H) chorda tympani.

Virtual temporal bones are generated by processing Micro-CT scans of human cadaveric temporal bones. A Micro-CT scan is a 3D volume of grey scale data, from which the temporal bone and the underlying anatomical structures are identified and segmented through a semi-automated process. The output of this step is a discretised 3D volume with labels to identify different structures. The structures are then rendered in the virtual operating space using a modified marching cubes algorithm [21]. This algorithm produces a surface mesh consisting of a set of triangles for each anatomical structure (and bone). Figure 3 illustrates the process of generating virtual models from microCT scans.

During a virtual surgery, the segment data is updated as material is removed. The area being drilled is re-rendered in real-time using the updated segment data. In addition, the simulator records the timestamp and location of each voxel that has been removed, making it possible to track the sequence in which material is removed. In addition, other metrics such as specimen and drill position, specimen orientation, and distance of the drill to anatomical structures are saved at a frequency of about 15Hz. This data can be used to recreate a surgery and identify which area of the bone is drilled during a given time interval.

B. Cochlear Implant Surgery

The operation undertaken to insert a cochlear implant consists of a few stages. First, a cortical mastoidectomy is performed to remove bone from the mastoid and uncover anatomical structure landmarks such as the dura, sigmoid sinus, and facial nerve. Then, the bone between the facial nerve and the chorda tympani (facial recess) is removed in a posterior tympanotomy. There are typically two approaches to cochlear implantation in the next stage: through the round window membrane or via a cochleostomy (an opening into the cochlea) [22].

Although there are benefits to both approaches, several studies have shown that for straight electrodes, the cochleostomy approach may result in less trauma [5], [6], [23]. As such, in our system, we consider cochleostomy as the default approach to cochlear implantation. Figure 4 shows the view of the temporal bone after the surgery has been conducted. Once this is achieved, the electrode is inserted into the cochlea through the cochleostomy.

III. Problem Formulation

A. Representation of Regions and Structures of Interest

To obtain the relevant areas, we recorded the procedure of an expert otologist performing a cochlear implant surgery on the simulator. The surgeon was asked to fully drill the facial recess and drill all possible locations for a cochleostomy, during which time, we noted the time intervals when each area was drilled. We then extracted the voxels corresponding to the facial recess and cochleostomy using the time intervals

(a) Micro-CT scan of a temporal bone.

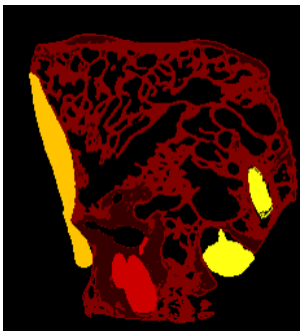

(b) Segmented volume: each anatomical structure is represented in a different colour.

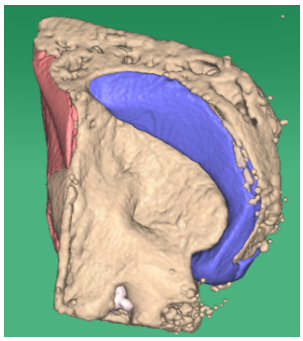

(c) Bone and anatomical structures rendered in 3D.

Figure 3: Generation of virtual models using MicroCT data.

and the timestamp data recorded by the simulator (see section II-A for details of timestamp data).

To fill holes and obtain the full masks for the facial recess and cochleostomy, we used morphological operations such as dilation and erosion [24]. Now, any voxels drilled in one of these areas can be identified by intersecting the drilled voxels with the area mask, in real-time if necessary, without the need to note time intervals. The cochlea is represented as a mesh of triangles as discussed in section II-A). Figure 5 shows an instance of a facial recess and cochleostomy drilling, along with the cochlea.

B. Considerations and Assumptions

Practical considerations in electrode insertion and assumptions made in the problem formulation are listed below. Details of their usage in the solution will be discussed in section IV.

- The cochlear implant electrode is a right circular cylinder with a radius r.
- The distance between the entry point of the electrode into the cochlea and the cochleostomy should be at most e_{thresh}.
- The distance between the entry point and the contact point of the electrode with the internal wall of the cochlea should be at least d_{thresh}.
- Any trajectories that are at a distance less than a given distance f_{thresh} at the facial recess and a distance c_{thresh} at the contact point of the cochlea are considered to be coincident.

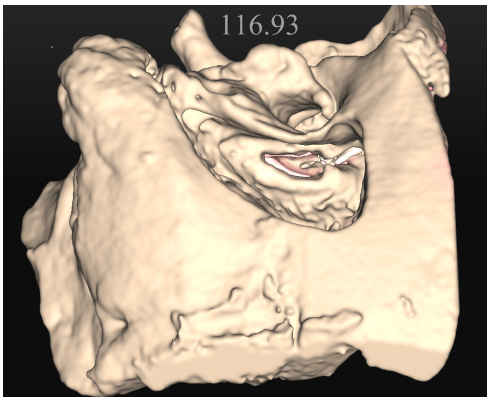

Figure 4: Cochlear implant surgery via cochleostomy.

IV. System Design

Once the drilled regions of the facial recess and cochleostomy are represented as a set of voxels and the cochlea is represented as a set of triangles (as discussed in section III-A), we calculate the resulting electrode insertion trajectories as follows. A graphical representation of the notations used in this section is given in figure 6.

A. Determination of Insertion Vectors

We generate all valid insertion vectors that pass through the drilled facial recess and cochleostomy, assuming that the electrode is a line vector with negligible width. To this end, we determine the lines going through all the drilled voxels in the facial recess and all those in the cochleostomy. We represent this set of lines L as:

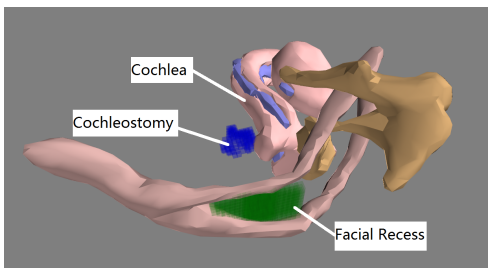

Figure 5: Representation of regions and structures of interest.

$$L = \bigcup_{i=1,j=1}^{n^F,n^C} P_i^F P_j^C \tag{1}$$

where, P^F and P^C are drilled points in the facial recess and the cocheostomy respectively, and n^F and n^C are the number of drilled voxels for these two regions. The notations of relevant points as well as their locations are illustrated in Figure 6.

We denote $P_i^F P_j^C$ as l_{ij} for simplicity. For any line $l_{ij} \in L$ we can define a point P_{ij} on it as follows:

$$P_{ij} = P_i^F + \lambda_{ij}\hat{u}_{ij} \tag{2}$$

where, λ_{ij} is a scalar parameter and $\hat{u}_{ij} = \frac{P_j^C - P_i^F}{\|P_j^C - P_i^F\|}$ is the unit vector on l_{ij}.

As discussed above, the cochlea is a closed surface represented by a mesh of triangles. Each triangle is represented by three vertices. The intersection point P_{ijk} between each line $l_{ij} \in L$, and the plane formed by each k^{th} triangle satisfies the following (triple product) equation, as it lies on the k^{th} plane.

$$[(T_{k2} - T_{k1}) \times (T_{k3} - T_{k1})] \cdot (P_{ijk} - T_{k1}) = 0 \tag{3}$$

where, T_{k1}, T_{k2}, and T_{k3} are the vertices of the k^{th} triangle in the surface mesh.

Solving equations 2 and 3, the scalar that represents the intersection point on the line l_{ij} can be obtained as:

$$\lambda_{ijk} = \frac{n_k \cdot (T_{k1} - P_i^F)}{n_k \cdot \hat{u}_{ij}} \tag{4}$$

where $n_k = (T_{k2} - T_{k1}) \times (T_{k3} - T_{k1})$ is the normal to the plane formed by the k^{th} triangle and λ_{ijk} is the scalar that defines the intersection point as: $P_{ijk} = P_i^F + \lambda_{ijk}\hat{u}_{ij}$.

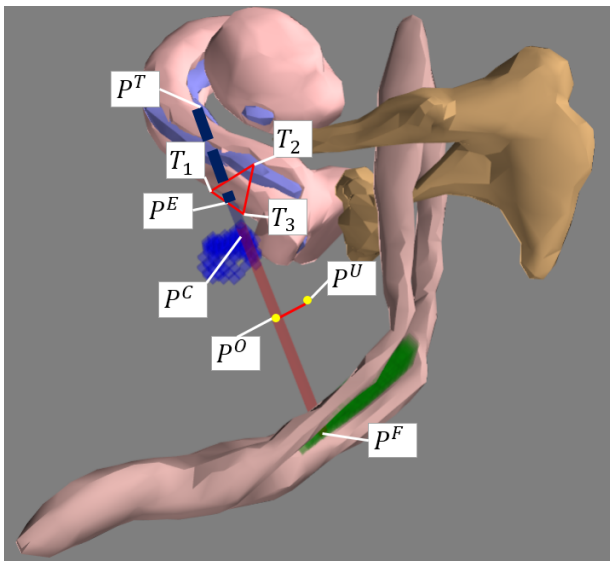

Figure 6: Notations and locations of relevant points.

Note that if the plane and the line under consideration are coplanar, the line is tangent to the surface of the cochlea and no unique intersection point exists. As we are not interested in tangent points, the k^{th} triangle is removed from further calculations for the ij^{th} line.

Although this calculation provides the intersection point between l_{ij} and the plane formed by the k^{th} triangle of the cochlea surface, it does not guarantee that the intersection point will be within the bounds of the triangle. Thus, to determine if an intersection point is within the k^{th} triangle or not, it is defined using barycentric coordinates as follows:

$$P_{ijk} = a_{ijk}T_{k1} + b_{ijk}T_{k2} + c_{ijk}T_{k3} \tag{5}$$

where, $[a_{ijk}, b_{ijk}, c_{ijk}]$ are the barycentric coordinates of the point P_{ijk} with respect to the triangle represented by the vertices T_{k1}, T_{k2}, and T_{k3}.

The barycentric coordinates for an intersection point P_{ijk} are obtained as shown in equation 6. If $0 \leq a_{ijk} \leq 1$, $0 \leq b_{ijk} \leq 1$, and $0 \leq c_{ijk} \leq 1$, P_{ijk} is within the bounds of the triangle (including on the edges and vertices).

$$[a_{ijk}\ b_{ijk}\ c_{ijk}]^T = [T_{k1} \mid T_{k2} \mid T_{k3}]^{-1} \cdot P_{ijk} \tag{6}$$

By rejecting the those P_{ijk} that are outside the bounds of the triangle, we obtain the set of intersection points for all $l_{ij} \in L$ with the cochlear surface. As the cochlea is a closed surface, multiple intersection points can exist for each line. The intersection point with the least distance from the j^{th} drilled point on the cochlea P_j^C, is the point where the electrode enters the cochlea (say P_{ij}^E). The intersection point with the second least distance is the point of contact of the electrode with the internal surface of the cochlea (say P_{ij}^T).

In practice, only those P_{ij}^E that are close to the cochleostomy are considered as valid entry points. Thus, we reject l_{ij} as a valid trajectory if the distance from P_{ij}^E to the cochleostomy is greater than a given threshold e_{thresh}. Further, depending on the type of electrode being used, for a valid trajectory, the distance between P_{ij}^E and P_{ij}^T should be greater than or equal to a threshold d_{thresh}. The remaining trajectories are those that are valid for an electrode with a negligible width.

B. Collision Detection with Undrilled Bone and Anatomical Structures

The next step is to consider the width of the electrode and remove those trajectories that collide with anatomical structures or undrilled bone voxels. To avoid checking voxels that are not close to the area under consideration, we define the areas that the electrode would occupy as that between (and around) the facial recess and cochleostomy masks using morphological operations such as dilation [24].

For each trajectory resulting from the previous step, we test if at least one of the undrilled voxels in the defined area fall within the radius of the electrode (r). As the

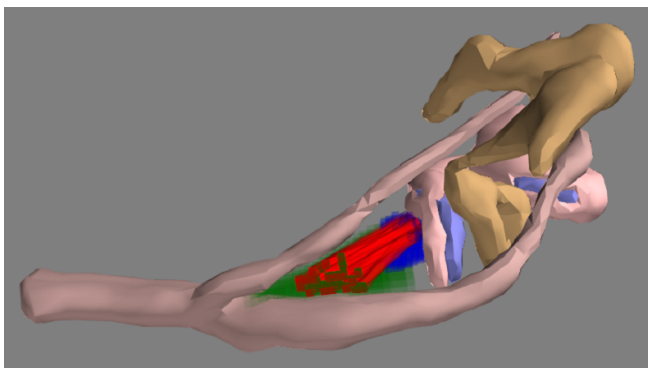

(a) Adequately drilled facial recess.

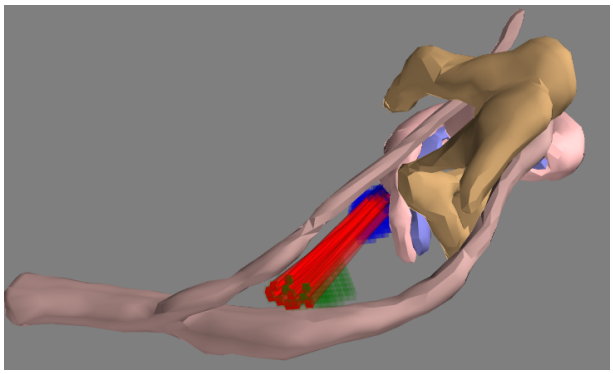

(b) Partially drilled facial recess.

Figure 7: Visualisation of valid electrode trajectories for a cochleostomy and two facial recess drillings.

orthogonal projection point from a given undrilled voxel is perpendicular to the unit vector $\hat{u}_{ij}$ of trajectory l_{ij}, the following equation is satisfied.

$$\hat{u}_{ij} \cdot \left(P_m^U - P_{ijm}^O\right) = 0 \tag{7}$$

where, P_m^U is the m^{th} undrilled voxel in the area of interest, and P_{ijm}^O is the orthogonal projection point of P_m^U on trajectory l_{ij}.

As the orthogonal projection point lies on l_{ij}, it also satisfies equation 2, giving us the scalar that represents it on l_{ij} as follows:

$$\lambda_{ijm} = \hat{u}_{ij} \cdot \left(P_m^U - P_i^F\right) \tag{8}$$

where λ_{ijm} the the scalar from which the orthogonal projection point can be obtained as $P_{ijm}^O = P_i^F + \lambda_{ijm} \cdot \hat{u}_{ij}$.

The orthogonal distance from the undrilled voxel P_m^U to the line l_{ij} can then be calculated as:

$$\mathrm{d}_{\mathrm{orth}}(P_m^U, l_{ij}) = \left\| P_m^U - P_{ijm}^O \right\| \tag{9}$$

If this distance is less than or equal to the electrode radius r, the undrilled voxel collides with the electrode, and thus makes the trajectory l_{ij} invalid.

C. Removal of Coincident Trajectories

Although all valid trajectories pertaining to a given combination of drilled facial recess and cochleostomy are found in the previous steps, some of them may be too close to each other to be considered separate trajectories. Thus, in this step, we determine how close each trajectory is to all the others at the end points (at the facial recess and contact points of the cochlea). If two trajectories l_p and l_q are coincident, they satisfy the following conditions.

$$\begin{aligned} \mathrm{coincident}(l_p, l_q) = &\left\| P_p^T - P_q^T \right\| \leq c_{thresh} \text{ AND} \\ &\left(\mathrm{d}_{\mathrm{orth}}(P_p^F, l_q) \leq f_{thresh} \text{ OR} \right. \\ &\left. \mathrm{d}_{\mathrm{orth}}(P_q^F, l_p) \leq f_{thresh}\right) \end{aligned} \tag{10}$$

where, $\mathrm{d}_{\mathrm{orth}}(P_p^F, l_q)$ is the orthogonal distance between the facial recess point P_p^F of trajectory l_p and any other trajectory l_q, calculated using equation 9. P_p^T and P_q^T are the contact points of the trajectories l_p and l_q with the internal wall of the cochlea respectively.

Once all the trajectories have been checked for coincidence with all the other trajectories, we remove those with the highest number of coincidences first and repeat the process until no trajectories that are coincident are left. The resulting list of trajectories satisfy all the required conditions for a given electrode, drilled facial recess, and cochleostomy.

Once all valid trajectories are calculated, they can be visualised alongside anatomical structures such as the facial nerve and cochlea to analyse their distribution. Quantitative measures such as the number of available trajectories can also be extracted. This form of analysis is useful in understanding the relationship between the amount of voxels drilled in the facial recess and the location and size of the cochleostomy with respect to anatomical variations.

V. Example Analysis

Here, we visualise and analyse the valid electrode trajectories for partially and fully drilled facial recesses when combined with the same cochleostomy on the same temporal bone specimen. The parameter values used in this calculation are: r=0.325mm, e_{thresh}=2mm, d_{thresh}=5.5mm, f_{thresh}=0.325mm, and c_{thresh}=0.1mm.

As can be observed in figure 7, the number of trajectories is reduced when the facial recess is not adequately drilled. For example, 203 valid trajectories are available for the case in 7a, while it is reduced to 110 in the case shown in 7b.

VI. Conclusion

We presented a method to visualise and analyse valid cochlear electrode trajectories for different temporal bone dissections. This is important in training cochlear implant surgery, as it allows the trainee to explore different strategies and observe their impact on the available electrode

trajectories. Further, as trainees are also able to visualise the relationship of the anatomical structures to the electrode trajectories, they are able to understand which strategy may be used in which situation. For example, on some anatomical variations, it may not be possible to find valid trajectories for straight electrodes through a cochleostomy. In such cases, alternative approaches such as insertion through the round window membrane or the use of a contoured electrode may be required.

In future work, we will implement this prototype system in our VR temporal bone surgery simulator to provide real-time visualisation and analysis of electrode trajectories (as well as haptic enabled electrode insertion simulation) to surgical trainees. We will validate its effectiveness in training cochlear electrode insertion through user studies of surgical residents.

ACKNOWLEDGMENT

This work was funded through an Australian Research Council Linkage grant in collaboration with Cochlear Ltd.

REFERENCES

[1] N. L. Cohen, "Cochlear implant candidacy and surgical considerations," *Audiology and Neurotology*, vol. 9, no. 4, pp. 197–202, 2004.

[2] A. Van Zon *et al.*, "Cochlear implantation for patients with single-sided deafness or asymmetrical hearing loss: a systematic review of the evidence," *Otology & Neurotology*, vol. 36, no. 2, pp. 209–219, 2015.

[3] P. L. Santa Maria *et al.*, "Hearing preservation surgery for cochlear implantation: a meta-analysis," *Otology & Neurotology*, vol. 35, no. 10, pp. e256–e269, 2014.

[4] R. J. MLA Briggs *et al.*, "Development and evaluation of the modiolar research array–multi-centre collaborative study in human temporal bones," *Cochlear implants international*, vol. 12, no. 3, pp. 129–139, 2011.

[5] X. Meshik *et al.*, "Optimal cochlear implant insertion vectors," *Otology & neurotology: official publication of the American Otological Society, American Neurotology Society [and] European Academy of Otology and Neurotology*, vol. 31, no. 1, p. 58, 2010.

[6] R. J. Briggs *et al.*, "Cochleostomy site: implications for electrode placement and hearing preservation," *Acta otolaryngologica*, vol. 125, no. 8, pp. 870–876, 2005.

[7] P. S. Roland, C. G. Wright, and B. Isaacson, "Cochlear implant electrode insertion: the round window revisited," *The Laryngoscope*, vol. 117, no. 8, pp. 1397–1402, 2007.

[8] Y. Shapira, A. A. Eshraghi, and T. J. Balkany, "The perceived angle of the round window affects electrode insertion trauma in round window insertion–an anatomical study," *Acta otolaryngologica*, vol. 131, no. 3, pp. 284–289, 2011.

[9] R. Torres *et al.*, "Variability of the mental representation of the cochlear anatomy during cochlear implantation," *European Archives of Oto-Rhino-Laryngology*, pp. 1–10, 2015.

[10] A. George and R. De, "Review of temporal bone dissection teaching: how it was, is and will be," *The Journal of Laryngology & Otology*, vol. 124, no. 02, pp. 119–125, 2010.

[11] A. Arora *et al.*, "Face and content validation of a virtual reality temporal bone simulator," *Otolaryngology–Head and Neck Surgery*, p. 0194599811427385, 2011.

[12] G. J. Wiet *et al.*, "Training otologic surgical skills through simulation-moving toward validation: a pilot study and lessons learned," vol. 1, no. 1, pp. 61–66, 2009.

[13] G. J. Wiet, D. Stredney, and D. Wan, "Training and simulation in otolaryngology," *Otolaryngologic Clinics of North America*, vol. 44, no. 6, pp. 1333–1350, 2011.

[14] A. Arora *et al.*, "Virtual reality simulation training in otolaryngology," *International Journal of Surgery*, vol. 12, no. 2, pp. 87–94, 2014.

[15] H. W. Francis *et al.*, "Technical skills improve after practice on virtual-reality temporal bone simulator," *The Laryngoscope*, vol. 122, no. 6, pp. 1385–1391, 2012.

[16] G. J. Wiet *et al.*, "Virtual temporal bone dissection system: Osu virtual temporal bone system," *The Laryngoscope*, vol. 122, no. S1, pp. S1–S12, 2012.

[17] Y. C. Zhao *et al.*, "Can virtual reality simulator be used as a training aid to improve cadaver temporal bone dissection? results of a randomized blinded control trial," *The Laryngoscope*, vol. 121, no. 4, pp. 831–837, 2011.

[18] P. Piromchai, A. Avery, M. Laopaiboon, G. Kennedy, and S. O'Leary, "Virtual reality training for improving the skills needed for performing surgery of the ear, nose or throat," *The Cochrane Library*, 2015.

[19] B. Copson, S. Wijewickrema, Y. Zhou, P. Piromchai, R. Briggs, J. Bailey, G. Kennedy, and S. O'Leary, "Supporting skill acquisition in cochlear implant surgery through virtual reality simulation," *Cochlear Implants International*, vol. 18, no. 2, pp. 89–96, 2017.

[20] C. Todd and F. Naghdy, "Virtual cochlear implant insertion for medical education," in *Eurohaptics Conference, 2005 and Symposium on Haptic Interfaces for Virtual Environment and Teleoperator Systems, 2005. World Haptics 2005. First Joint*. IEEE, 2005, pp. 505–506.

[21] S. Wijewickrema, I. Ioannou, and G. Kennedy, "Adaptation of marching cubes for the simulation of material removal from segmented volume data," in *Proceedings of the 26th IEEE International Symposium on Computer-Based Medical Systems*. IEEE, 2013, pp. 29–34.

[22] A. A. Mikulec, "The temporal bone: A manual for dissection and surgical approaches," 2007.

[23] O. F. Adunka *et al.*, "Scala tympani cochleostomy ii: topography and histology," *The Laryngoscope*, vol. 117, no. 12, pp. 2195–2200, 2007.

[24] R. M. Haralick, S. R. Sternberg, and X. Zhuang, "Image analysis using mathematical morphology," *IEEE transactions on pattern analysis and machine intelligence*, no. 4, pp. 532–550, 1987.